ELSEVIER

Chemical Engineering Journal 88 (2002) 141–150

Chemical Engineering Journal

www.elsevier.com/locate/cej

Radial solids flow structure in a liquid–solids circulating fluidized bed

Ying Zheng[1], Jing-Xu Zhu*, Narenderpal S. Marwaha, Amarjeet S. Bassi

Department of Chemical and Biochemical Engineering, The University of Western Ontario, London, Ont., Canada N6A 5B9

Received 23 March 2001; received in revised form 15 November 2001; accepted 15 November 2001

Abstract

Radial flow structure was studied using a fiber-optical probe in a 7.6 cm ID and 3.0 m high liquid–solids circulating fluidized bed (LSCFB). Radial solids holdup profiles were obtained at four different heights for glass beads and plastic beads of mean diameters 508 and 526 μm, respectively. The results show that local suspension densities are greater near the wall than in the center of the riser for both types of particles, confirming the existence of the radial non-uniformity. Under the same cross-sectional average solids holdup, the radial profiles of solids holdup are the same for each type of particle system under different operating conditions, but the light particles (plastic beads) show a flatter radial profile than the relatively heavier particles (glass beads). Discussion on the solids acceleration explains why a non-uniform axial profile in the LSCFB only exists for very heavy particles and only under limited operating conditions.

Keywords: Radial non-uniformity; Solids holdup distribution; Solids acceleration; Liquid–solids circulating fluidized bed

1. Introduction

Liquid–solids circulating fluidized beds (LSCFBs) have a number of attractive features which make them suitable to processes where liquid–solids contacting is important [1,2]. The ability to accommodate widely differing particulate materials with high liquid throughputs, uniform temperature, effective liquid–solids contacting and independent control of solids holdup by varying the external recycle rate of particles are advantages which have been shown to benefit some chemical processes [3] and bioprocesses [1,4]. For example, LSCFB is an excellent candidate for the continuous recovery of protein from unclarified whole broth where the adsorption and desorption (regeneration) of proteins can be carried out separately in the downcomer and the riser in a continuous mode with the ion exchange particles circulated between the two columns [4,5]. The desorption buffer and the feed broth are used to fluidize the particles in the riser (for desorption) and the downcomer (for adsorption), with the riser operated in the circulating fluidization regime and the downcomer in the conventional fluidization regime. The de-proteinized broth is discarded from the downcomer top and the buffer with desorbed proteins is collected at the riser top after separating the regenerated particles from the effluent in a liquid–solid separator.

In the past few years, there have been some limited studies on the hydrodynamics in the riser of the LSCFBs and its overall operation: when the liquid velocity is low, the riser is operated in the extensively studied conventional fluidization regime, which is considered to be a homogenous fluidization where particles are uniformly distributed in both the axial and radial directions in the dense phase [6]. When the liquid velocity is increased beyond the particle terminal velocity, the liquid fluidized bed in the riser transfers into the high-velocity circulating fluidization regime and eventually reaches the dilute liquid transport [1,7–9]. In the circulating fluidization regime, some studies [7,10] have reported uniform distribution of solids holdup in the axial direction of the riser and have used this criterion to demarcate the transition to the circulating fluidization regime. However, recent study by Zheng et al. [9] suggested that particle density has a great influence on the axial profile of solids holdup and showed that heavy particles lead to non-uniform axial distribution, dense at the bottom and dilute at the top of the riser, in the initial zone of the circulating fluidization regime where superficial liquid velocity is relatively low (such non-uniformity disappears with further increase in liquid velocity). Because such relatively small non-uniformity only appears under a narrow range of operating conditions and only when very heavy particles are used [9], the axial flow structure in LSCFB should be considered completely

* Corresponding author. Tel.: +1-519-661-3807; fax: +1-519-661-2441.
E-mail address: zhu@uwo.ca (J.-X. Zhu).
[1] Currently at Department of Chemical Engineering, University of New Brunswick, Canada.

1385-8947/02/$ – see front matter
PII: S1385-8947(01)00294-7

Nomenclature

G_s	solids circulation rate (kg/(m^2 s))
H	axial location (m)
r	radial coordinate (mm)
R	radius of the riser (mm)
U_a	auxiliary liquid velocity (solids-free basis) (cm/s)
U_{cr}	critical transition velocity of the circulating fluidization (cm/s)
U_g	superficial gas velocity (m/s)
U_l	total liquid velocity (solids-free basis) (cm/s)
U_s	particle circulation rate expressed as superficial particle velocity ($=G_s/\rho_s$) (cm/s)
U_t	particle terminal velocity (cm/s)

Greek letters

ε	cross-sectional average voidage
ε_s	local solids holdup
$\bar{\varepsilon}_s$	cross-sectional average solids holdup

different from the consistently non-uniform axial flow in the gas–solids circulating fluidized bed (GSCFB). In GSCFB, the non-uniform axial flow structure, with solids holdup and other related variables all varying with the axial position of the riser, results from the solids acceleration [11,12]. Due to the large density difference between gas and solids, the solids acceleration section can take a substantial length of the riser, separating the riser into a developing flow region and a developed flow region in GSCFB. For LSCFB, however, the developing flow region at the riser bottom is insignificant given the small solids/liquid density ratio. Only for very heavy particles and only at low liquid fluidization velocities, a small developing flow region appears at the riser bottom, leading to some axial non-uniformity [9].

The radial flow structure in the liquid–solids circulating fluidization regime has only been investigated by Liang et al. [13]. They pointed out that unlike the conventional liquid–solids fluidized bed, the radial distribution of bed voidage is not uniform for glass beads, using an electrical conductivity probe in the liquid–solids circulating fluidization regime. However, this work was carried out with only one type of particles under limited operating conditions. On the other hand, radial non-uniformity may affect the reactant concentration distribution, mass transfer and ultimately, reactant conversions. Therefore, information on radial flow structure is crucial to reactor design and process optimization.

Comparing with LSCFBs, GSCFBs have received much more attention and the non-uniformity of radial gas and solids flow structure has been studied more thoroughly by many researchers (e.g. [14,15]). Herb et al. [14] suggested that there may be a universal radial bed voidage distribution profile for a given time-averaged solids concentration over the cross-section. This was supported by Tung et al. [16] and Zhang et al. [15] with tests using different particles conducted at different superficial gas velocities and solids flow rates in different risers. The radial distribution of bed voidage can therefore be considered as a function of the average cross-sectional bed voidage only. To investigate whether a similar universal radial flow distribution also exists in LSCFB, systematical experiments are needed to study the radial flow structure for different types of particles and over a wider operating range.

The investigation reported in this work was undertaken in an effort to examine the radial distribution of solids holdup under wide range of operating conditions and to test the effect of particle density on the flow structure. Attempts were also made to study the flow development along the riser. At last, the LSCFBs are compared with GSCFBs.

2. Experimental

The set-up of the LSCFB system is shown schematically in Fig. 1. The system mainly consists of a Plexiglas riser column of 7.62 cm ID and 3 m in height, a liquid–solids separator, a device for measuring the solids flow rate and a storage vessel serving as the solids reservoir. This riser was connected to the 0.2 m ID Plexiglas storage vessel through a solids returning pipe at the top and a solids feeding pipe at the bottom. At the bottom of the riser, there are two distributors: the main liquid distributor, made of seven stainless steel tubes occupying 19.5% of the total riser cross-sectional area and extending 0.2 m into the riser and the auxiliary liquid distributor, a porous plate with 4.8% opening area at the base of the riser.

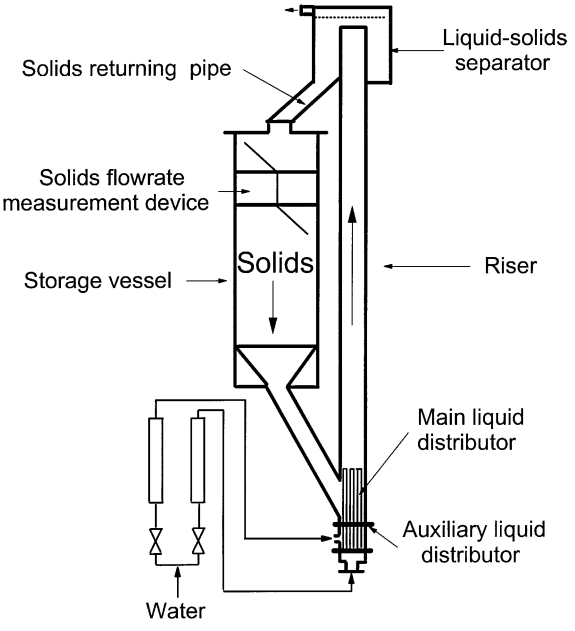

Fig. 1. The schematic diagram of the LSCFB apparatus.

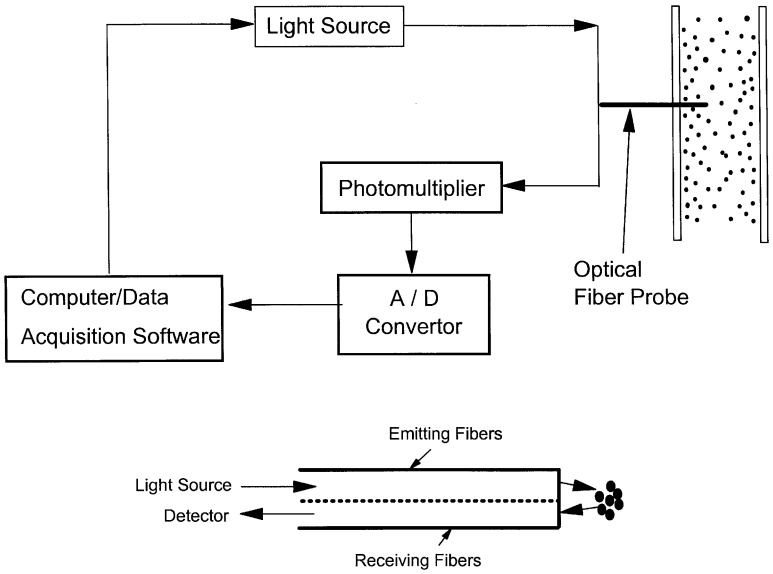

Fig. 2. The fiber-optical probe system for solids holdup measurement.

The liquid and solids flow rates can be controlled independently by adjusting the main and the auxiliary liquid flow rates. The auxiliary liquid stream controls the quantity of the particles recirculating from the storage vessel to the riser: when the auxiliary flow was set to zero, no particles could enter the riser and no continuous particle circulation could be formed. Introducing the auxiliary liquid flow, solids did not begin to flow immediately. Only when the auxiliary liquid flow reached a threshold flow rate, solids began to flow. After that, additional liquid added to the riser bottom caused more particles to enter the riser. Particles introduced into the riser bottom are carried up the top of the riser by the total liquid flow (the main liquid flow plus the auxiliary liquid flow) and separated by the large cone-based cylindrical liquid–solids separator at the top. Liquid is then returned to the liquid reservoir and the particles are returned to the particle storage vessel after passing through the solids flow-rate measuring device.

The local solids holdup was measured using an optical fiber solids concentration probe. Fig. 2 shows schematically the fiber-optic system used in this work. The optical fiber probe is made of two bundles of quartz fibers encased in a 3.8 mm ID stainless steel probe tip, containing 8000 emitting and receiving quartz fibers, each 15 μm in diameter. One bundle of fibers act as light projectors carrying light from a source and projecting it onto the passing swarm of particles. The other interspersed bundle acts as light receivers transmitting the light reflected by the particles to a phototransistor which converts the light into an electrical signal. An amplifier increases the resulting signal to a voltage range 0–5 V, after which the signal is fed to a personal computer via an A/D converter. The relative error of the probe measurement is 1/256 of the full measurement range, so that the accuracy is 0.2% for ε_s measurements. For the details of this probe, please refer to [17].

The calibration of this probe for the two liquid–solids systems were carried out on site. With the fluidized bed operated in the conventional particulate regimes, where the solids holdup is the considered homogeneous in both the axial and the radial direction, the output voltage signal from the probe is calibrated against the solids holdup data obtained from pressure gradient measurements. Linear relationship was found between the voltage signal and the solids holdup for each type of the particles.

All experiments were carried out at ambient temperature. Tap water was used as the fluidizing liquid. The physical properties of the two types of particles used are listed in Table 1. In each run, local solids holdup was measured at different radial positions by traversing the probe horizontally, after the LSCFB unit was brought to a steady operation. In early measurements, the probe was traversed from one wall to the other and no significant asymmetry was found in the radial holdup profile. Therefore, measurements in this work were taken only at one side of the riser, at seven radial locations between the center and the wall at $r/R = 0.00$, 0.40, 0.58, 0.71, 0.82, 0.92 and 0.99. The same procedure was repeated for different solids flow rates and liquid velocities at different levels. For each measurement location, the column section from about 0.3 m above to 0.3 m below the probe was wrapped with a black plastic sheet to prevent external light from penetrating into the riser and interfering with the measurements.

Table 1
Physical properties of solid particle

Particles	d_p (μm)	ρ_s (kg/m^3)	U_t (cm/s)
Polycarbonate (plastic) beads	526	1100	1.0
Glass beads	508	2490	5.9

3. Results and discussion

3.1. Radial solids holdup distribution

The radial distribution of solids holdup in the LSCFB is non-uniform for both types of particles studied: glass beads and plastic beads. Fig. 3 shows the radial holdup distributions for the two types of particles under the same solids flow rate and different liquid velocities, up to 42 cm/s. The non-uniform distribution of radial solids holdup is established after the fluidized bed enters the liquid–solids circulating fluidization regime (e.g. $U_l = 10$ cm/s in Fig. 3a). The radial non-uniformity of solids holdup, dilute in the center and dense near the wall, can be clearly seen in the LSCFB. In the center, the solids holdup has a rather homogeneous distribution and is lower than the cross-sectionally averaged solids holdup; near the wall, solids holdup increases quickly until a maximum is reached at the wall. There is no clear boundary between the dilute and dense regions so that a core annulus structure does not really exist. Increasing liquid velocity, the non-uniformity is increased as can be seen in Fig. 3a when the liquid velocity increases from $U_l =$ 10 to 14 cm/s. Further increasing liquid velocity, the radial non-uniformity of the solids holdup decreases significantly (e.g. $U_l = 28$ cm/s in Fig. 3a), an indication that the bed begins the transition from the circulating fluidization regime to the dilute transport regime [7].

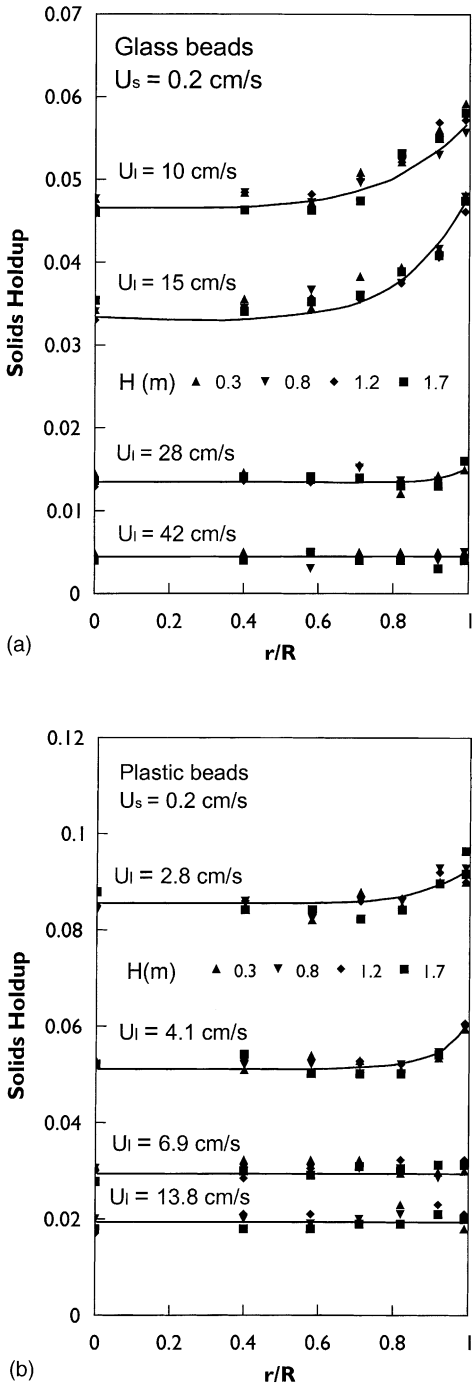

Fig. 3. The radial distributions of solids holdup at four bed levels at different superficial liquid velocities for (a) glass beads and (b) plastic beads.

Fig. 4 shows the variation of the radial solids holdup distributions with solids flow rate under the same normalized liquid velocity (superficial liquid velocity divided by the particle terminal velocity of each type) for each type of particles. For a wide range of operating conditions, it is seen that the increase of the particle circulation rate (in terms of the superficial solids velocity) increases the average solids holdup and the radial non-uniformity of the solids holdup for the two types of particles. This increase of the non-uniformity with increasing solids flow rate can also be seen in Fig. 5, where the four lines show the increasing trends of the local solids holdups at four different radial positions with increasing solids flow rate. Increasing U_s, the local solids holdup at each radial position increases but the increase of the local solids holdup in the center is slower than that near the wall. For example, the local solids holdup increases from 0.010 to 0.062 at the axis, whereas at the wall it nearly reaches 0.082 when the solids flow rate increases from 0.04 to 0.60 cm/s. From Fig. 4, it is also noted that the increase of the average solids holdup with increasing solids flow rate for plastic beads is faster than that for glass beads. For example, the average solids holdup of glass beads increases from 0.037 to 0.052 when U_s rises from 0.2 to 0.4 cm/s. In the plastic beads system, the average solids holdup has a larger increase from 0.039 to 0.062 with a smaller increase of U_s from 0.040 to 0.073 cm/s. In addition, under the same solids flow rate, plastic beads have a steeper radial flow structure due to the higher average solids holdup.

3.2. Radial profile along the riser

From Fig. 3, it can also be seen that there is little difference between the radial distributions of solids holdup at the lower section ($H = 0.3$ m), the middle section ($H = 0.8$ and 1.2 m) and the upper section ($H = 1.7$ m) of the riser for the given liquid velocities and solids circulating rates. This suggests that under a specific operating condition, there

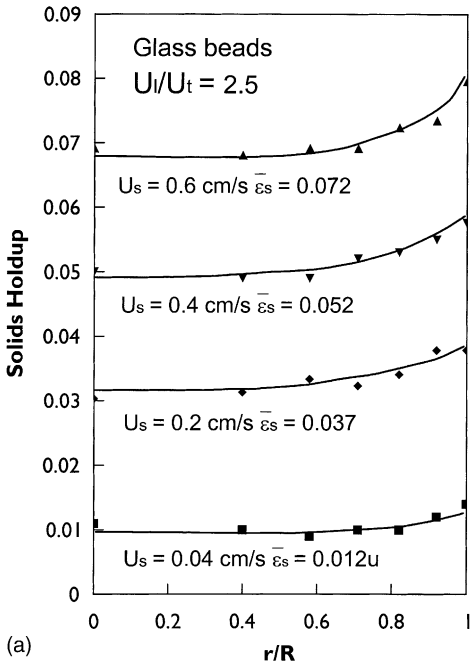

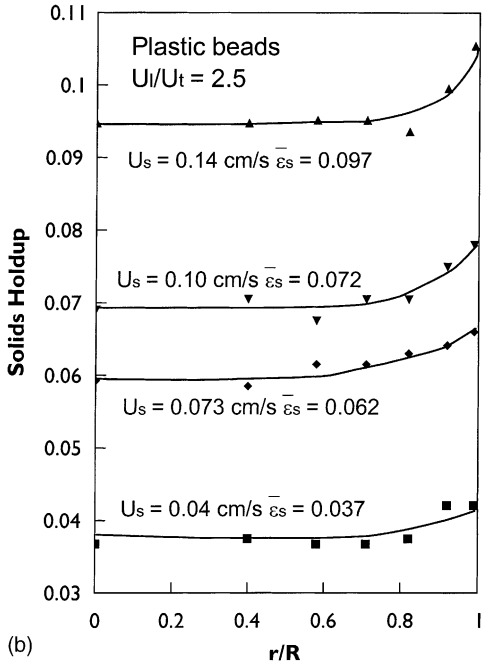

Fig. 4. Radial profiles of solids holdup at the level $H = 0.8$ m for different solids flow rates for (a) glass beads and (b) plastic beads at the same normalized liquid velocity, $U_l/U_t = 2.5$.

exists a similar flow structure along the height of the circulating fluidized bed, indicating a rather uniform axial flow structure for the relatively light particles (e.g. glass beads and plastic beads) in the LSCFB. Figs. 6 and 7 show the cross-sectionally averaged solids holdup under different liquid velocities and particle circulation rates. It is seen that the axial solids holdup distribution is uniform for both plastic

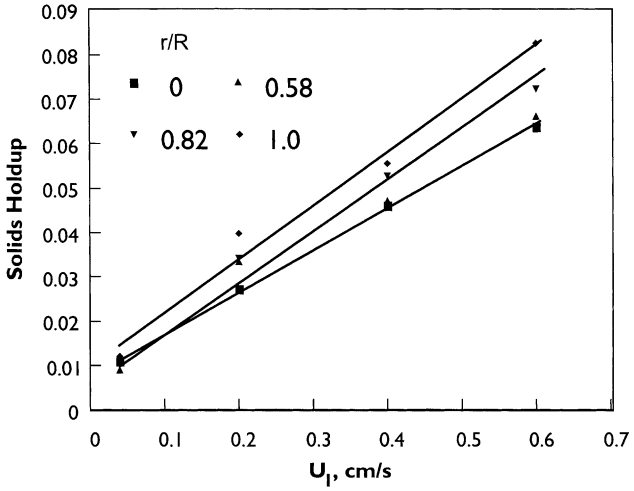

Fig. 5. Variation of local solids holdups at four radial locations with the solids flow rate for $U_l = 15$ cm/s and $H = 0.8$ m for glass beads.

beads and glass beads systems, although the radial distribution is non-uniform. Liang et al. [7] and Zheng et al. [9] have also reported such uniform axial solids holdup distributions in their studies.

When the system is operated at low liquid velocity ($U_l = 10$ cm/s) but high particle circulation rate ($U_s = 0.4$ and 0.6 cm/s), a minor deviation from the axial uniform particle distribution is observed in the glass beads system as shown in Fig. 6 (but no deviation is observed in the plastic beads system in Fig. 7). The average solids holdups of the glass beads at the bottom (and also at the top for $U_s = 0.6$ cm/s) of the riser are slightly higher than that of the middle section. Increasing the liquid velocity, this minor non-uniformity disappears. Generally, particles at the bottom of the riser have a solids velocity of about zero upon entering the riser and need some time to be accelerated to the normal solids velocity by the upflowing liquid, with the flow transferring from the developing flow region to the fully developed flow region. Heavier particles need more time (and therefore more distance) to accelerate [18]. At low liquid velocity, heavier glass beads develop slower so that a axial non-uniformity can be identified. This will be discussed in detail later (see Section 3.4).

The radial holdup distributions plotted in Fig. 8 are corresponding to the data shown in Fig. 6 for a solids flow rate of 0.6 cm/s and liquid velocities of 10 and 15 cm/s. Under the operating condition where there exists a non-uniform axial distribution ($U_s = 0.6$ cm/s, $U_l = 10$ cm/s), the radial non-uniformity of the solids holdup distribution at the bottom ($H = 0.35$ m) and top ($H = 1.70$ m) sections of the riser (where the average solids holdup is higher) is greater than that at the middle ($H = 0.80$ and 1.25 m) section (Fig. 8a). This is expected since denser particle suspension leads to greater radial non-uniformity of the solids holdup distribution (as shown in Fig. 4). Increasing liquid velocity to 15 cm/s, the parabolic curves which represent the radial

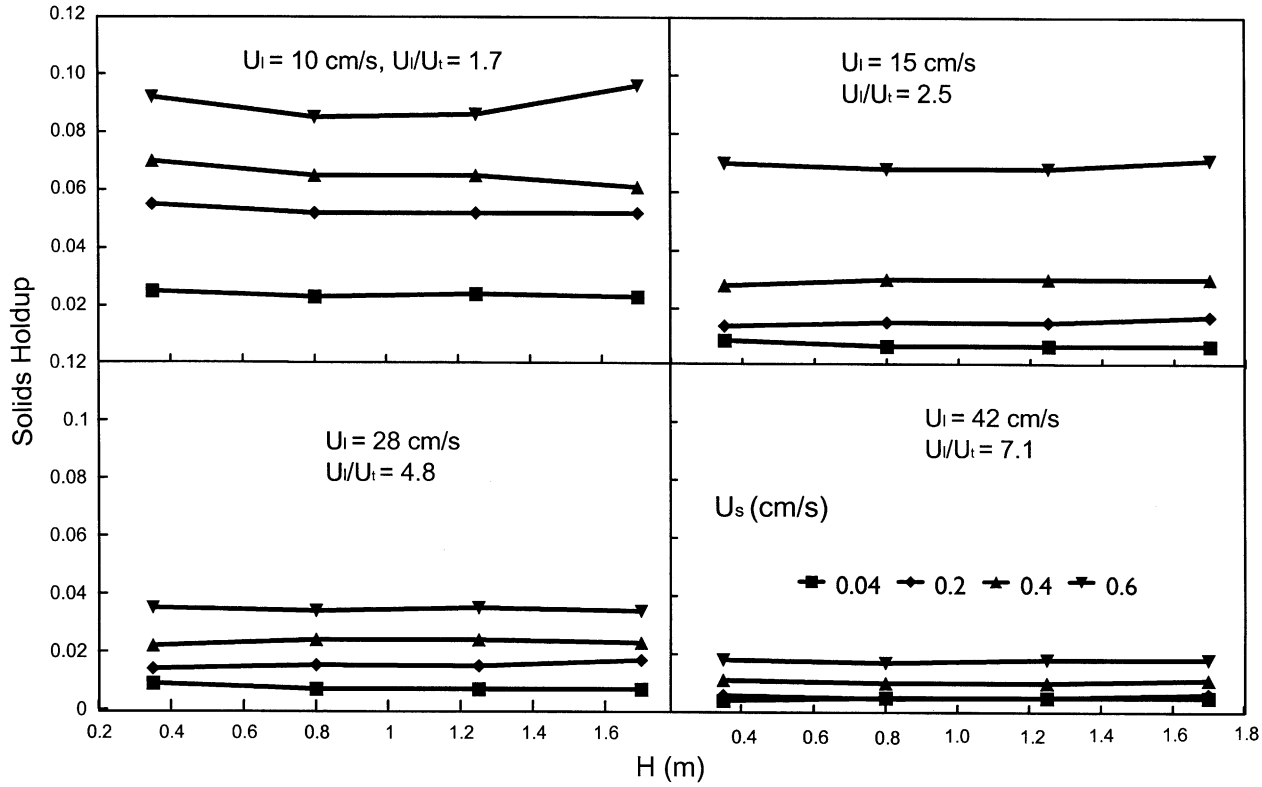

Fig. 6. Axial distributions of solids holdup under different operating conditions for glass beads.

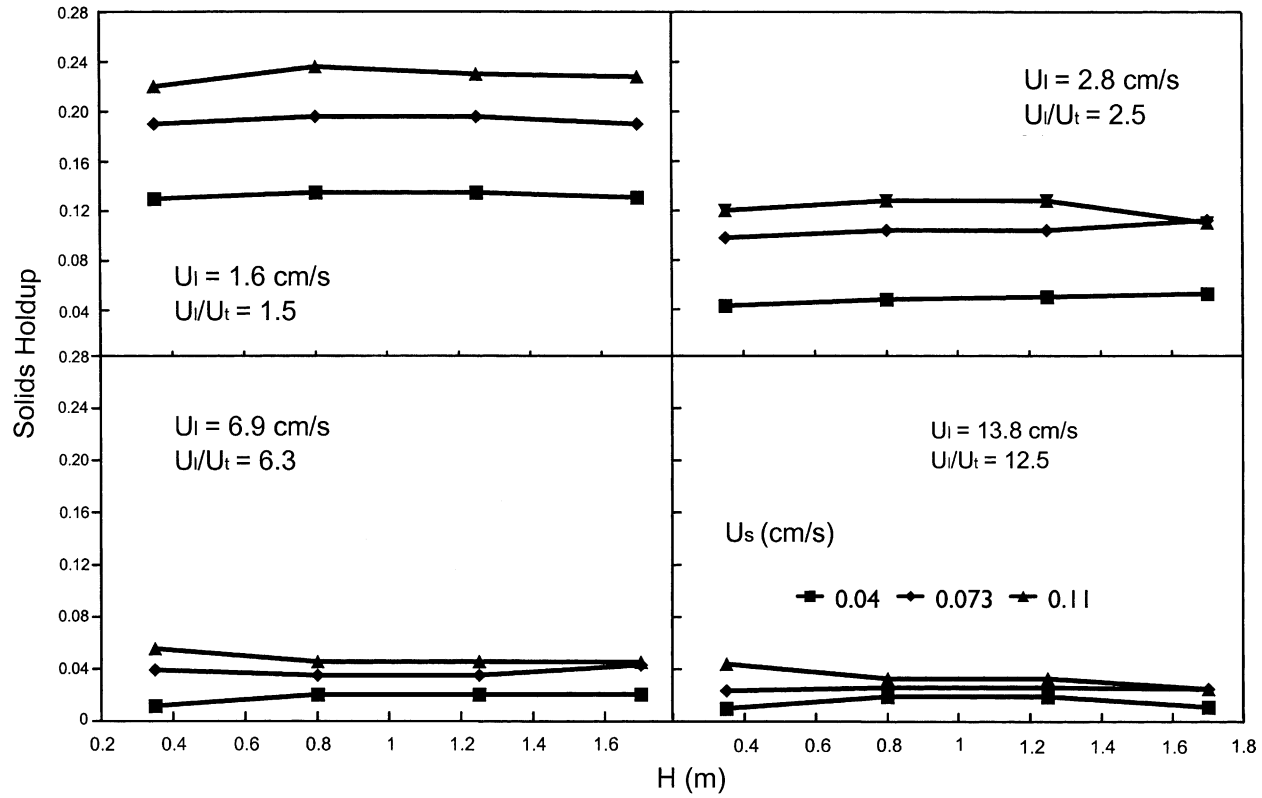

Fig. 7. Axial distributions of solids holdup under different operating conditions for plastic beads.

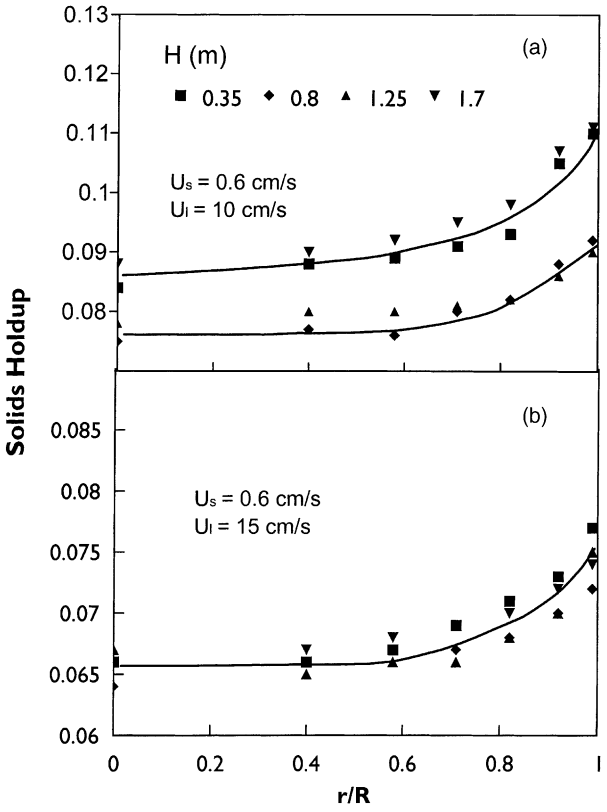

Fig. 8. Radial profiles of solids holdup at four levels for $U_s = 0.6$ cm/s and $U_l = 10$ and 15 cm/s for glass beads.

solids holdup distributions at the four axial levels coincide together well and follow the same pattern (Fig. 8b), indicating that the same radial non-uniformity of the solids holdup at the four levels in the riser (and therefore a uniform axial profile) have been achieved. Since the deviation in the glass beads system can be observed only under a narrow range of operating conditions and is not significant, the glass beads system can still be considered as uniform in the axial particle distribution when the liquid–solids system enters the liquid–solids circulating fluidized regime.

3.3. Radial solids holdup distribution under the same average solids holdup

Adjusting the main and the auxiliary liquid velocities, the same cross-sectional average solids holdup can be obtained under different operating conditions. Fig. 9 shows the radial distributions of the solids holdup under the same average solids holdup but different total liquid flow rates and solids flow rates (for glass beads) are almost identical, although variations in either the liquid velocity or the solids flow rate alone can significantly affect the radial holdup profile. This may be explained by the momentum balance of particles in the riser. Given the radial distribution of the liquid velocity, higher in the center and lower near the wall, particles in the center of the riser obtain higher solids velocity. To maintain momentum balance over the cross-sectional area, a net transfer of particles from the center to the wall region is necessary so that the typical parabolic profile of radial

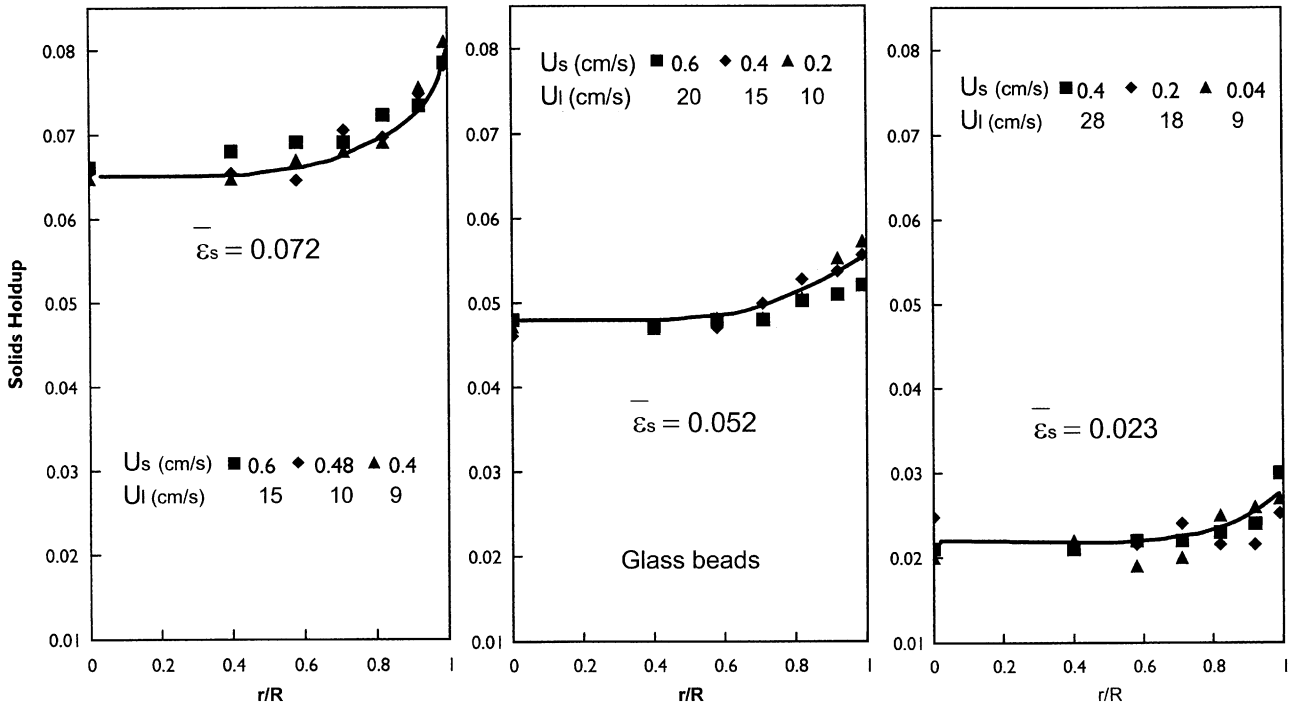

Fig. 9. Radial profiles of solids holdup under the same cross-sectional average solids holdups for glass beads.

solids holdup distribution is obtained [19]. When the solids flow rate increases while the liquid velocity remains the same, more particles are expected to be present in the riser and the increased number of particles should be distributed in the same manner, less in the center and more at the wall. Obviously, the radial profile becomes steeper according to the distribution of the additional particles. Correspondingly, increasing liquid velocity gives the opposite result. When the increase in solids flow rate is accompanied by an increase in liquid velocity to maintain the same cross-sectional average solids holdup, the increase and the reduction of solids holdup, due to the increases of the solids flow rate and liquid velocity, respectively, can be kept the same so that the radial profile of solids holdup remains the same. From Fig. 9, it is also seen that the parabolic profile of the radial solids concentration distribution flattens out with the decrease of the average solids holdup. Similar results have also been observed in the plastic beads system. Following this line of reasoning, for each type of particles, there may exist a universal radial profile of solids holdup for any given cross-sectional average solids concentration in the LSCFB system, which is also reported by Liang et al. [13]. The similar conclusion was also obtained in the GSCFB systems [15,16].

Fig. 10 shows the radial distribution of solids holdup for glass beads and plastic beads of similar size under the same cross-sectional average solids holdup. Although parabolic profiles are observed for both types of particles, the local radial particle distribution for the light plastic beads system appears to feature a somewhat more uniform contour under the same cross-sectional average solids holdup. Comparing with the glass beads system, a slightly higher average solids holdup in the center and a larger dilute center region are seen in the plastic beads system, giving a flatter parabolic profile in the lighter plastic beads system. This is different from the GSCFB where the radial voidage profile is not significantly affected by the solid materials for Geldart A particles, as concluded by Zhang et al. [15].

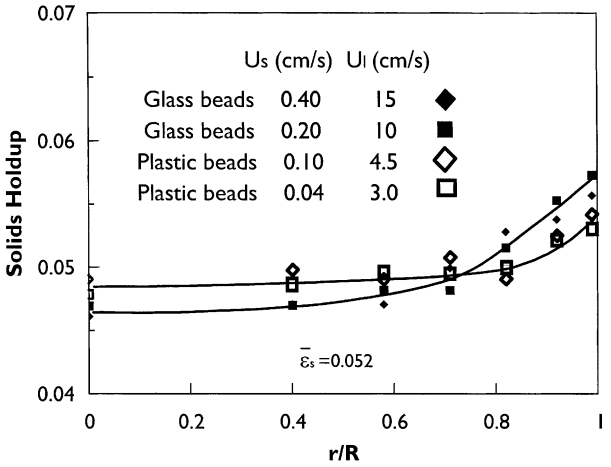

Fig. 10. Comparison of the radial solids holdup profiles for glass beads and plastic beads under the same cross-sectional average solids holdup ($\bar{\varepsilon}_s = 0.052$) at $H = 0.8$ m.

3.4. Solids acceleration

Figs. 3, 4, 6 and 7 show that the axial profile of solids holdup in the LSCFB is uniform although minor denser regions are observed at the bottom under some specific operating conditions (Fig. 6). An essential element concerning the axial flow structure in the LSCFB, that should be taken into account but has not been reported in the previous reports, is the solids acceleration. In the LSCFB, the particles circulated in the unit are usually fed into the riser bottom horizontally or downward so that the velocity of the particles at the bottom of the riser is either zero or negative. The particles must first be accelerated by the upflowing liquid flow to a point where the drag force exerted by the liquid flow equals the gravitational force. Beyond this point, the particle velocity becomes constant. Therefore, two regions exist in the riser, the developing flow region and the fully developed flow region. Within the developing flow region located at the lower portion of the riser, the particles are accelerated along with the decrease of the solids holdup. When the solids velocity becomes constant, the solids holdup remains unchanged too, an indication that the liquid–solids flow enters into the fully developed flow region. Thus, the denser region at the bottom of the riser as shown in Fig. 6 can be considered as the developing flow region, within which the solids acceleration is achieved.

The length of the developing flow region, also called the acceleration length, varies with the operating conditions. The acceleration length for the same type of particles decreases with decreasing solids flow rate and/or increasing fluid velocity [12]. It is shown in Fig. 6, in which the minor axial non-uniformity disappears when the liquid velocity increases from 10 to 15 cm/s or the solids flow rate decreases from 0.4 to 0.2 cm/s. Particle density is another factor affecting the acceleration length in the riser. Comparing with glass beads, the density of plastic beads is much lower. This leads to a much shorter acceleration length and thus the acceleration region is hardly identifiable in the LSCFB under all operating conditions shown in Fig. 7. The result that the acceleration length is increased with particle density explains the phenomenon reported by Zheng et al. [9] that the axial holdup distribution of the very heavy steel shots is non-uniform in the initial circulating fluidization zone where the liquid velocity is relatively low. In addition, the result here is also consistent with the previous reports in GSCFBs [12,18].

Comparing with the gas–solids system, the acceleration length (or the developing flow region) in an LSCFB is much shorter. This is reasonable since the solid–fluid density ratio is a key factor in affecting the solids acceleration. In the LSCFB where the solid–liquid density ratio is very low, the acceleration length is insignificant compared to the entire length of the riser column and disappears when the liquid velocity is increased and/or the solids flow rate is reduced, even in the very heavy steel shots system [9]. On the contrary, the acceleration region in the GSCFB,

where the solid–gas density ratio is very high, often takes up one-third to two-third of the riser length or even the entire riser, leading to the distinct non-uniform distribution of dense bottom and dilute top regions [12,18].

The somewhat higher average solids holdup at the top of the riser under some conditions is likely to be due to the influence of the exits structure. At the high solids flow rate ($U_S = 0.6$ cm/s, $U_l = 10$ cm/s), more particles rebound back at the exit so that the solids holdup of the top section is increased. However, the magnitude of these deviations at both the top and the bottom section of the riser is low and the deviations happen only under very limited operating conditions. Therefore, the axial average solids holdup for the relative light particles studied here can be properly considered as uniform along the riser.

3.5. Comparison with the gas–solids system

The radial particle distribution in LSCFBs is also much more uniform than that in GSCFBs. Fig. 11 shows the comparison of some results obtained in this work with those reported by Zhang et al. [15] for a GSCFBs under the same cross-sectional average solids holdup. The decrease in the solids holdup from the wall to the axis in the liquid–solids system is only about 0.025 while in the gas–solids system it reaches 0.26, 10 times as large as in the liquid–solids system. The fluid–solids density ratio and the viscosity of the fluid medium are likely to be the key elements to generate the difference. Due to much higher liquid–solids density ratio and the much higher viscosity of liquid in the LSCFB, particles are easier to accelerate so that the particles at the wall essentially flow upwards although the particle velocity there is lower than that in the center. From this viewpoint, it is not surprising that, in the GSCFB, large quantity of particles in the vicinity of the wall are often observed to flow downward. According to Qi and Farag [19], particle concentration must be higher near the wall where the particle velocity is lower to satisfy the momentum balance across a cylindrical boundary at a given radial position. Comparing the movements of particles near the wall in the LSCFBs and the GSCFBs, it is clear that much higher particle concentration should be present at the wall region of the GSCFB in order to maintain the momentum balance. Therefore, a steeper parabolic profile of particle distribution exists in the GSCFB system.

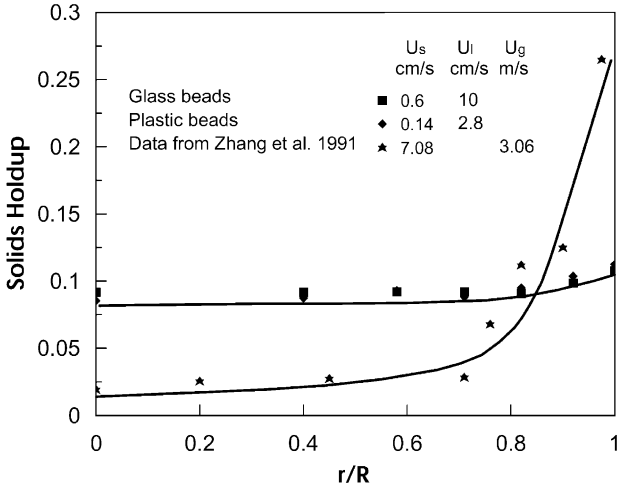

Fig. 11. Comparison of the radial solids holdup profiles in LSCFBs and GSCFBs under the same cross-sectional average solids holdup ($\bar{\varepsilon}_S = 0.095$).

4. Conclusion

An optical fiber probe was used to measure the local particle distribution at four levels in the riser of an LSCFB at different liquid velocities and solids flow rates. In the radial direction of the riser, non-uniformity exists in the solids holdup distribution, with high solids holdup near the wall. The non-uniformity increases with the increase of solids flow rate and the decrease of liquid velocity. The similar radial profiles of solids holdup measured at different bed levels indicate uniform flow structure along the axial direction. Particle density is an important factor to affect the flow structure: heavier particles lead to a steeper radial profile of solids holdup and a more visible acceleration region. However, the flow structure in both the axial and radial directions in the LSCFB is more homogeneous compared to that in the GSCFBs.

Acknowledgements

Financial supports from the Natural Sciences and Engineering Research Council of Canada, and from the University of Western Ontario through the President Scholarship of Graduate Studies to the Ying Zheng is gratefully acknowledged.

References

[1] J.-X. Zhu, Y. Zheng, D.G. Karamanev, A.S. Bassi, (Gas)–liquid–solid circulating fluidized beds and their potential applications to bioreactor engineering, Can. J. Chem. Eng. 78 (2000) 82–94.
[2] Y. Jin, J.-X. Zhu, Z.-Q. Yu, Novel configurations and variants, in: J.R. Grace, A.A. Avidan, T.M. Knowlton (Eds.), Circulating Fluidized Bed, Blackie, London, 1997, pp. 525–567 (Chapter 6).
[3] W.-G. Liang, Z.-Q. Yu, Y. Jin, Z.-W. Wang, Y. Wang, M. He, E. Min, Synthesis of linear alkylbenzene in a liquid–solids circulating fluidized bed reactor, J. Chem. Technol. Biotechnol. 62 (1995) 98–102.
[4] Q. Lan, J.-X. Zhu, A.S. Bassi, A. Margaritis, Y. Zheng, Continuous protein recovery using a liquid–solids circulating fluidized bed ion exchange system: modelling and experimental studies, Can. J. Chem. Eng. 78 (2000) 858–866.
[5] C. Lan, A.S. Bassi, J.-X. Zhu, A. Margaritis, Continuous protein recovery using a liquid–solid circulating fluidized bed ion exchanges, *AIChE* J. 2002, in press.

[6] J.-P. Couderc, Incipient fluidization and particulate systems, in: J.F. Davidson, R. Clift, D. Harrison (Eds.), Fluidization, 2nd Edition, Academic Press, London, 1985, pp. 1–46 (Chapter 1).
[7] W.-G. Liang, S.-L. Zhang, J.-X. Zhu, Y. Jin, Z.-Q. Yu, Z.-W. Wang, Flow characteristics of the liquid–solid circulating fluidized bed, Powder Technol. 90 (1997) 95–102.
[8] Y. Zheng, J.-X. Zhu, The onset velocity of a liquid–solid circulating fluidized bed, Powder Technol. 114 (2000) 244–251.
[9] Y. Zheng, J.-X. Zhu, J. Wen, S. Martin, A. Bassi, A. Margaritis, The axial hydrodynamic behavior in a liquid–solid circulating fluidized bed, Can. J. Chem. Eng. 77 (1999) 284–290.
[10] K. Kuramoto, K. Tanaka, A. Tsutsumi, K. Yoshida, T. Chiba, Macroscopic flow structure of solid particles in circulating liquid–solid fluidized bed riser, J. Chem. Eng. Jpn. 31 (1998) 258–265.
[11] K.S. Lim, J.-X. Zhu, J.R. Grace, Hydrodynamics of gas fluidization, Int. J. Multiphase Flow Suppl. 21 (1995) 140–193.
[12] W.-X. Huang, J.-X. Zhu, J.H. Parssinen, Experimental study on solids acceleration length in a long CFB riser, Chem. Eng. Technol., 2002, in press.
[13] W.-G. Liang, J.-X. Zhu, Y. Jin, Z.-Q. Yu, Z.-W. Wang, J. Zhou, Radial non-uniformity of flow structure in a liquid–solid circulating fluidized bed, Chem. Eng. Sci. 51 (1996) 2001–2010.
[14] B. Herb, K. Tuzla, J.C. Chen, Distribution of solid concentrations in circulating fluidized bed, in: J.R. Grace, L.W. Shemilt, M.A. Bergougnou (Eds.), Fluidization VI, Engineering Foundation, New York, 1989, pp. 65–72.
[15] W. Zhang, Y. Tung, F. Johnsson, Radial voidage profiles in fast fluidized beds of different diameters, Chem. Eng. Sci. 46 (1991) 3045–3052.
[16] Y. Tung, J. Li, M. Kwauk, Radial voidage profiles in a fast fluidized bed, in: M. Kwauk, D. Kunii (Eds.), Fluidization'88: Science and Technology, Science Press, Beijing, 1988, pp. 139–146.
[17] H. Zhang, P.J. Johnston, J.-X. Zhu, H.I. de Lasa, M.A. Bergougnou, A novel calibration procedure for a fiber-optic concentration probe, Powder Technol. 100 (1998) 260–272.
[18] D. Bai, Y. Jin, Z. Yu, The length of particle acceleration region in fast fluidized beds (in Chinese), Chem. Reaction. Eng. Technol. 6 (1990) 34–39.
[19] C.-M. Qi, I.-H. Farag, Lateral particle motion and its effect on particle circulation distribution in the riser of CFB, AIChE Symp. Ser. 89 (296) (1993) 73–80.